Innovation in metallurgical industrial and laboratory equipment, technologies and materials / **Инновации в металлургическом промышленном и лабораторном оборудовании, технологиях и материалах**

UDC 621.74.045
DOI 10.17073/0368-0797-2024-4-463-470

Original article
Оригинальная статья

Stress-strain state of ceramic shell mold during formation of spherical steel casting in it. Part 2

V. I. Odinokov, A. I. Evstigneev, E. A. Dmitriev, A. N. Namokonov, A. A. Evstigneeva, D. V. Chernyshova

Komsomolsk-na-Amure State University (27 Lenina Ave., Komsomolsk-on-Amur, Khabarovsk Territory 681013, Russian Federation)

diss@knastu.ru

Abstract. The paper presents the results of numerical calculations of the solution to the problem of modeling the process of possible cracking in a spherical shell mold when pouring liquid steel into it and cooling the solidifying casting. The numerical scheme of the axisymmetric problem and the algorithm for its solution were given in Part 1. The crack resistance is estimated by magnitude of the normal stresses in the ceramic shell during its co-cooling with a solidifying casting. The results detailed analysis considered: fields of displacement, stresses, and temperatures both on spherical surface and in growing crust of solidified metal. The solution took into account the change in the shear modulus of the mold material from temperature, and an assessment of this refinement was given. The problem was solved in two ways. The first – with a constant shift modulus of the shell mold; the second – with its temperature-dependent shift modulus. There is a significant difference between these variants in terms of magnitude of the normal stresses arising in the shell mold. The authors analyzed resistance of the shell mold spherical geometry to external influences from its support filler and filling funnel. The problem of determining the contact and free surfaces at the boundary of the shell mold and support filler was solved. The results are presented graphically in the form of diagrams of stresses and temperatures over the studied area in its different sections and time intervals for cooling of the growing metal crust. The role of compressive normal stresses σ_{22}, σ_{33} on the surface of contact of the shell mold with liquid metal at the initial moment of cooling on probability of cracking in a spherical mold is shown. The level of strain-stress state in a spherical shell mold when cooling a steel casting in it is significantly determined by dependence of shift modulus of the shell mold on temperature.

Keywords: investment casting, shell mold, stressed state, modeling, cracking

Acknowledgements: The research was supported by the Russian Science Foundation, grant No. 24-29-00214, https://rscf.ru/project/24-29-00214/.

For citation: Odinokov V.I., Evstigneev A.I., Dmitriev E.A., Namokonov A.N., Evstigneeva A.A. Chernyshova D.V. Stress-strain state of ceramic shell mold during formation of spherical steel casting in it. Part 2. *Izvestiya. Ferrous Metallurgy*. 2024;67(4):463–470. https://doi.org/10.17073/0368-0797-2024-4-463-470

Напряженно-деформированное состояние керамической оболочковой формы при формировании в ней стальной шарообразной отливки. Часть 2

В. И. Одиноков, А. И. Евстигнеев, Э. А. Дмитриев, А. Н. Намоконов, А. А. Евстигнеева, Д. В. Чернышова

Комсомольский-на-Амуре государственный университет (Россия, 681013, Хабаровский край, Комсомольск-на-Амуре, пр. Ленина, 27)

diss@knastu.ru

Аннотация. В статье приведены результаты численного решения задачи по моделированию процесса возможного трещинообразования в оболочковой форме (ОФ) шарообразной конфигурации при заливке в нее жидкой стали и охлаждении затвердевающей отливки. Численная схема осесимметричной задачи и алгоритм решения были приведены в части 1. Трещиностойкость оценивается

по величине нормальных напряжений в керамической ОФ в процессе ее совместного охлаждения с затвердевающей отливкой. При детальном анализе результатов были учтены поля перемещений, напряжений, температур как в сферической ОФ, так и в нарастающей корочке затвердевшего металла. При решении учитывалось изменение модуля сдвига материала формы от температуры, и была дана оценка этого уточнения. Задачу решали двумя способами. Первый – с постоянным модулем сдвига ОФ; второй – с модулем сдвига ОФ, зависящим от температуры. Между этими вариантами есть существенная разница в величине нормальных напряжений, возникающих в ОФ. Авторы проанализировали стойкости ОФ сферической геометрии от внешних воздействий со стороны опорного наполнителя (ОН) оболочковой формы и заливочной воронки. Была решена задача по определению контактной и свободной поверхностей на границе ОФ и ОН. Результаты решения задачи представлены графически в виде эпюр напряжений, температур по исследуемой области в разных ее сечениях и временных интервалах охлаждения ОФ и нарастающей корочки металла. Показана роль сжимающих нормальных напряжений σ_{22}, σ_{33} на поверхности соприкосновения ОФ с жидким металлом в начальный момент охлаждения на вероятность трещинообразования в сферической форме. Уровень напряженно-деформированного состояния в сферической ОФ при охлаждении в ней стальной отливки существенно определяется зависимостью модуля сдвига ОФ от температуры.

Ключевые слова: литье по выплавляемым моделям, оболочковая форма, напряженное состояние, моделирование, трещинообразование

Благодарности: Исследование выполнено за счет гранта Российского фонда № 24-29-00214, https://rscf.ru/project/24-29-00214/.

Для цитирования: Одиноков В.И., Евстигнеев А.И., Дмитриев Э.А., Намоконов А.Н., Евстигнеева А.А., Чернышова Д.В. Напряженно-деформированное состояние керамической оболочковой формы при формировании в ней стальной шарообразной отливки. Часть 2. *Известия вузов. Черная металлургия*. 2024;67(4):463–470. https://doi.org/10.17073/0368-0797-2024-4-463-470

Introduction

Previous studies on the influence of the stress-strain state (SSS) on the crack resistance of shell molds (SM) during the pouring of liquid metal and subsequent cooling with the solidifying casting were conducted using shell molds for investment casting (IC) in the form of risers with both cylindrical and spherical (sump) shapes. Numerous theoretical and experimental investigations have been carried out to identify the features of the SSS in ceramic shell molds and the resulting castings in investment casting. These studies examined various factors, including the materials used in the investment models [1; 2], the shape and geometry of the SM [3; 4], the mold wall thickness [5; 6], the mold material [7; 8], the geometry of the castings [9 – 11], methods for testing mold strength, and more [12; 13].

Mathematical modeling of these processes has also been presented in other works, covering modeling methods [14], research [15 – 17], numerical modeling [18 – 20], specialized mathematical models [21 – 23], and software tools [24; 25].

The production of spherical and globular IC castings, and consequently the resistance of the SM to cracking during the formation of such castings, is of both scientific and practical interest. The materials in this study are focused on addressing this issue.

In [26], the general approach to constructing a mathematical model for determining the SSS and temperature in an SM during the cooling of a spherical casting was presented, along with the numerical scheme and algorithm for solving the problem using developed software packages [27; 28]. This study presents the results of theoretical and numerical research aimed at solving the outlined problem.

Main body

In [26], the general problem of cooling a spherical casting in a shell mold was described.

Fig. 1 illustrates the computational scheme of the process under study, considering axial symmetry (where the angle α defines the size of the gating window, and the angle φ defines the extent of the SM's coverage by the supporting filler (SF)).

Initial date

Geometric parameters: $S = 5$ mm, $R_1 = 20$ mm.

Time intervals $\Delta\tau_n$: 0.1; 1.0; 2.0; 4.0; 5.0; 5.0; 5.0; 10.0; 10.0; 1.0; 2.0; 5.0; 1.0; 1.0; 3.0; 3.0; 5.0; 10.0; 10.0 s; the friction parameter on surface S_3 (Fig. 1) is $\psi = 0.001$.

Domain partitioning: $N_1 \times N_2 = 10 \times 30$.

Accepted physical parameters of the cast steel at a temperature of $\theta > 1000$ °C ($\theta^*_м = 1500$ °C): $G = 1000$ kg/mm^2 (shear modulus); $\alpha = 12 \cdot 10^{-6}$ °C^{-1} (coefficient of linear expansion); $\lambda = 0.0298$ W/(mm·°C) (thermal conductivity coefficient); $L = 270 \cdot 10^3$ J/kg (latent heat of fusion); $C = 444$ J/(kg·°C) (specific heat capacity); $\gamma = 7.80 \cdot 10^{-6}$ kg/mm^3 (density); $\theta_s = 1450$ °C (solidification temperature).

Physical properties of the ceramic mold: $G_m = 2910$ kg/mm^2; $\alpha = 0.51 \cdot 10^{-6}$ °C^{-1}; $\lambda = 0.000812$ W/(mm·°C); $C = 840$ J/(kg·°C); $\gamma = 2.0 \cdot 10^{-6}$ kg/mm^3.

Some theoretical studies [29] have shown that during the cooling of steel in an SM with α angles of 10 and 30° and $\varphi = (180° - \alpha)$, significant compressive stresses σ_{22} and σ_{33} can occur, potentially exceeding the compressive strength of the ceramic material. When $\alpha = 30°$, the stresses σ_{ii}, $i = 2, 3$ are slightly lower in absolute value

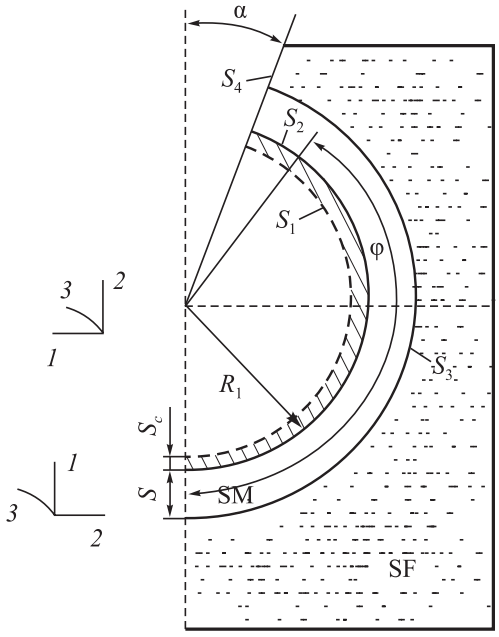

Fig. 1. Calculation scheme of a spherical ceramic shell mold molded in support filler and filled with liquid metal, taking into account axial symmetry:
LM – liquid metal; TM – solid metal; SM – shell mold; SF – support filler; S_1 – inner contact surface of liquid and solidified metal; S_2 – inner contact surface of solidified metal and shell mold; S_3 – outer surface of shell mold; S_4 – free surface of the end face of casting cup; R_1 – radius of spherical casting; S – thickness of shell mold; S_T – thickness of solidified metal crust; α – slope angle of funnel; φ – angle of enclosing surface of shell mold with a support filler

Рис. 1. Расчетная схема шарообразной ОФ, заформованной в опорный наполнитель и залитой жидким металлом, с учетом осевой симметрии:
LM – жидкий металл; TM – твердый металл; SF – оболочковая форма; TM – опорный наполнитель; S_1 – внутренняя поверхность контакта жидкого и затвердевшего металла; S_2 – внутренняя поверхность контакта затвердевшего металла и оболочковой формы; S_3 – внешняя поверхность оболочковой формы; S_4 – свободная поверхность торца литниковой чаши ОФ; R_1 – радиус шарообразной отливки; S – толщина оболочковой формы; S_T – толщина корочки затвердевшего металла; α – угол наклона литниковой воронки; φ – угол охвата поверхности оболочковой формы опорным наполнителем

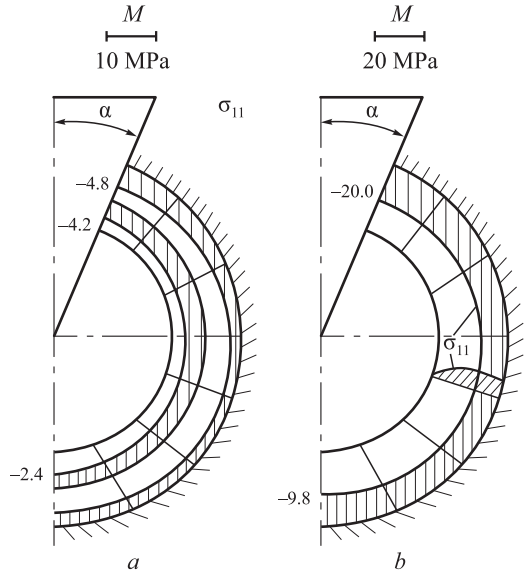

Fig. 2. Diagrams of normal stresses σ_{11} in shell mold at α = 10° and time of casting cooling 7.1 s (*a*) and 51.1 s (*b*)

Рис. 2. Эпюры нормальных напряжений σ_{11} в ОФ при α = 10° при времени охлаждения отливки 7,1 с (*a*) и 51,1 с (*b*)

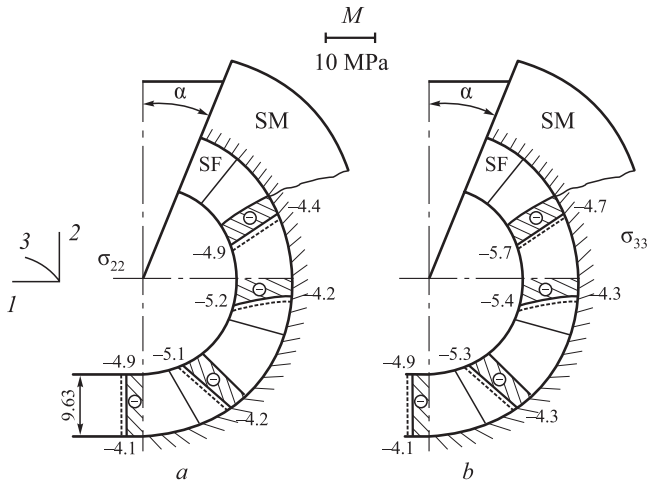

Fig. 3. Diagrams of normal stresses σ_{22} (*a*) and σ_{33} (*b*) in forming metal crust at α = 30° (solid lines) and α = 10° (dashed lines) and time of casting cooling 60.1 s

Рис. 3. Эпюры нормальных напряжений σ_{22} (*a*) и σ_{33} (*b*) в образующей корочке металла при α = 30° (сплошные линии) и α = 10° (штриховые линии) и времени охлаждения отливки 60,1 с

than at α = 10°. Fig. 2 shows the distribution of normal stresses σ_{ii} in the SM at α = 10°: (*a*) after 7.1 s of cooling, (*b*) after 51.1 s.

Fig. 3 illustrates the distribution of stresses σ_{22} and σ_{33} in the solidified metal shell after 60.1 s of cooling; solid lines represent the distributions at α = 30°, while dashed lines represent those at α = 10°.

The values of σ_{22} and σ_{33} on the surface adjacent to the liquid metal are greater (in magnitude) than on the surface of the SM, which is explained by the constant shear modulus G_m of the forming solid metal (1000 kg/mm^2), independent of temperature. As in the SM, the stresses σ_{22} and σ_{33} are compressive, and at α = 10°, they are higher than at α = 30°.

Fig. 4, *a* shows the distribution of stresses σ_{11} in the solidified metal skin after 60.1 s. The stresses σ_{11} are compressive throughout the cross-section: solid lines indicate σ_{11} at α = 30°, while dashed lines show them at α = 10°.

Fig. 4, *b* shows the growth curves of the skin thickness (S) and the stress σ_{33} over time. As the angle α increases, the normal stresses decrease slightly (in magnitude).

Further increasing α is unnecessary, as the metal skin continues to grow with only minor changes in normal stresses.

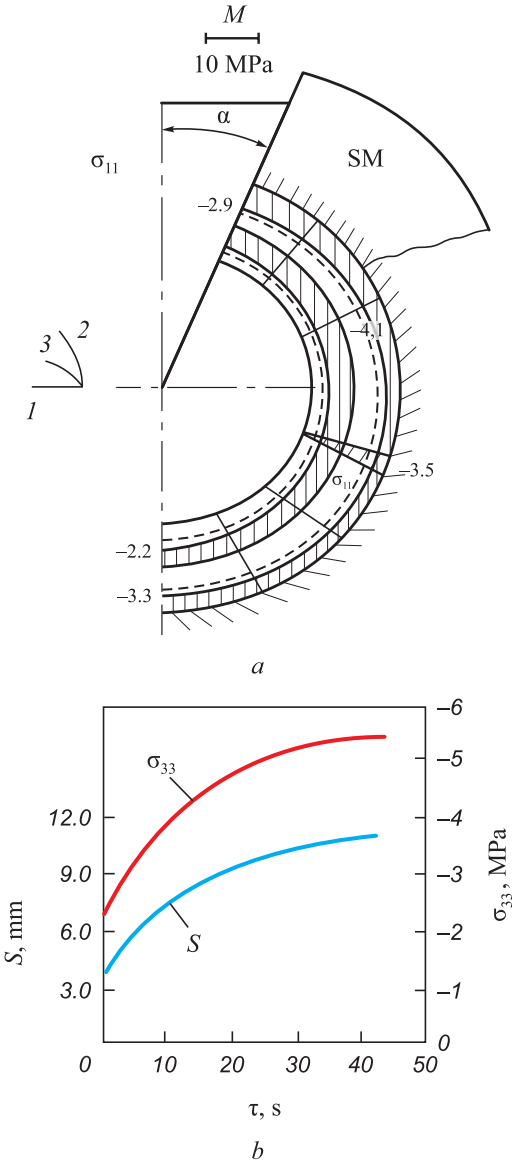

Fig. 4. Diagrams of normal stresses σ_{11} (*a*) in crystallized metal crust after casting cooling for 60.1 s and growth curves of metal crust (*S*) and stresses σ_{33} (*b*) with cooling time

Рис. 4. Эпюры нормальных напряжений σ_{11} (*a*) в закристаллизовавшейся корочке металла через время охлаждения отливки 60,1 с и кривые роста величины корочки металла (*S*) и напряжений σ_{33} (*b*) со временем охлаждения

The results were obtained assuming a constant (average) shear modulus for the SM (G_m).

As indicated in [29], the temperature in the SM adjacent to the solidifying metal is very high (around 1300 °C). At this temperature, the ceramic is practically in a softened state, meaning the shear modulus in this area will be much lower than the average value of G_m for the shell mold. We will use experimental data (Fig. 5) obtained in [30] from testing ceramic samples made from a binder material ($SiO_2 + MgPO_4$).

Approximating the results presented in Fig. 5, we obtain:

$$G_m = 6412 - 6.37\theta, \text{ kg/mm}^2 \text{ for } 300\ ^\circ\text{C} < \theta < 1000\ ^\circ\text{C};$$

$$G_m = 40 \text{ kg/mm}^2 \text{ for } \theta \geq 1000\ ^\circ\text{C};$$

$$G_m = 4500 \text{ kg/mm}^2 \text{ for } \theta < 300\ ^\circ\text{C}.$$

The results of the solution with a temperature-dependent shear modulus of the SM are shown in Fig. 6 at $\alpha = 10°$ as distributions of σ_{ii}, $i = 1, 2, 3$ for $\tau = 1.12$ s (solid lines); $\tau = 7.12$ s (dashed lines).

During thermal shock and cooling at $\tau = 1.12$ s, the stresses σ_{22} and σ_{33} have the highest values (in absolute terms) in the SM's contact zone with the metal, but they change sharply with cooling time. All normal stresses are compressive. The stresses σ_{33} in the forming skin ($S = 6$ mm) after $\tau = 7.12$ s are shown in Fig. 7.

With further cooling, the stresses σ_{ii} decrease.

The most critical period for failure is the initial cooling phase ($0 < \tau < 8$ s) (Fig. 6).

Figs. 8 and 9 show the calculation results for $\alpha = 30°$, $\tau = 1.12$ s (solid lines); $\tau = 7.12$ s (dashed lines).

As seen, the pattern is approximately the same, but the values of σ_{ii}, $i = 1, 2, 3$ are slightly lower than at

$SiO_2 + MgPO_4$

T	*E*	*Et*/*E*20	*G*, MPa	Vol. expansion coefficient
20	11250000000	1.0000	45,000	4.44444 E–06
100	11250000000	1.0000	45,000	4.44444 E–06
200	11250000000	1.0000	45,000	4.44444 E–06
300	11250000000	1.0000	45,000	4.44444 E–06
400	9642857143	0.8571	38,571	5.18519 E–06
500	8437500000	0.7500	33,750	5.92593 E–06
600	5625000000	0.5000	22,500	8.88889 E–06
700	4218750000	0.3750	16,875	1.18519 E–05
800	2596153846	0.2308	10,385	1.92593 E–05
900	1687500000	0.1500	6750	2.96296 E–05
1000	96428571	0.0086	386	5.18519 E–04
1100	61363636	0.0055	245	8.14815 E–04

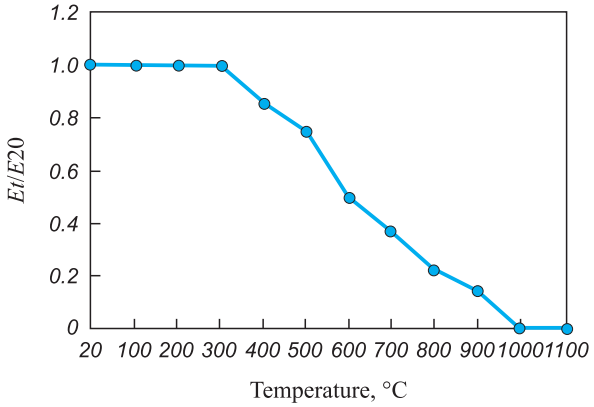

Fig. 5. Experimental data on tests of ceramic samples made of a binder ($SiO_2 + MgPO_4$)

Рис. 5. Экспериментальные данные при испытании керамических образцов, выполненных из связующего материала ($SiO_2 + MgPO_4$)

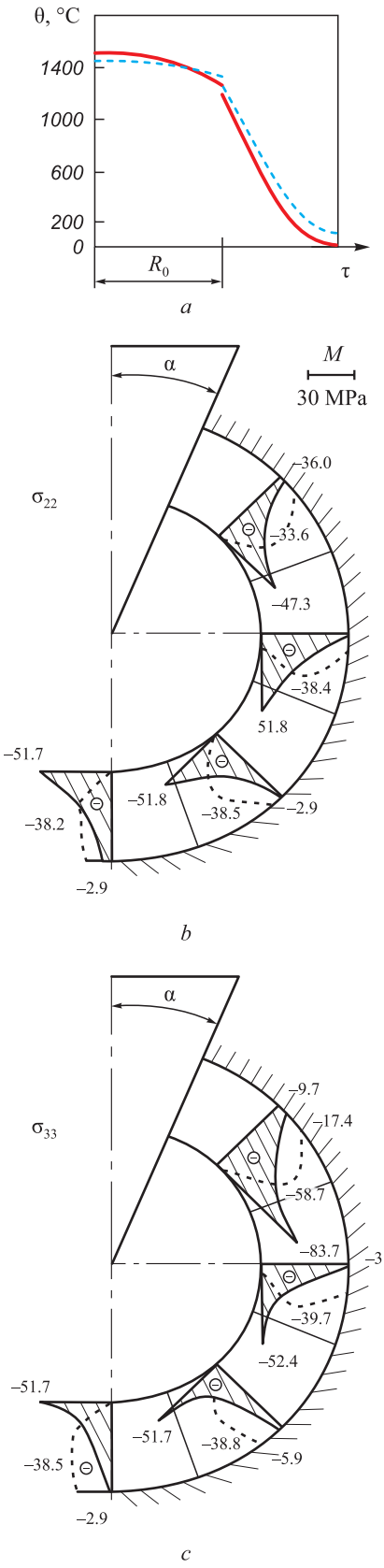

Fig. 6. Temperatures field (*a*), diagrams of normal stresses σ_{22} (*b*) and σ_{33} (*c*) in ceramic mold at time of casting cooling 1.12 s (——) and 7.12 s (– – –)

Рис. 6. Поле температур (*a*), эпюры нормальных напряжений σ_{22} (*b*) и σ_{33} (*c*) в ОФ при α = 10° и времени охлаждения отливки 1,12 с (——) и 7,12 с (– – –)

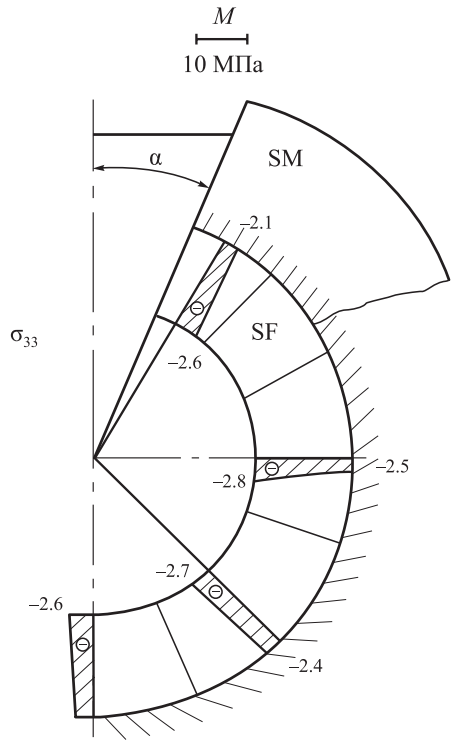

Fig. 7. Diagrams of normal stresses σ_{33} in resulting metal crust (S = 6 mm) at time of casting cooling 7.12 s

Рис. 7. Эпюры нормальных напряжений σ_{33} в образующейся металлической корочке (S = 6 мм) при времени охлаждения отливки 7,12 с

α = 10°, and small tensile stresses σ_{22} and σ_{33} have even appeared in the SM at the interface with the SF (Fig. 8). In the metal skin (S = 6 mm) after τ = 7.12 s, the stresses σ_{33} are shown (Fig. 9), which are also lower than at α = 10° (Fig. 3, *b*).

Further cooling shows that normal stresses decrease, and the distributions of σ_{ii} for τ = 32.12 and 52.12 s are close to each other.

Regarding the effect of the cylindrical SM material on its durability, these results were presented in previous works by the authors, where in the case under consideration, the most critical factor for potential crack formation in the SM is the tensile normal stresses σ_{22} in the outer layer of the shell, which is in contact with the supporting filler.

Considering the temperature dependence of the shear modulus in the SM significantly affects the stress-strain state during the cooling of the steel casting within it. Under the given external conditions for the metal cooling process in a spherical SM, its durability at the initial moment of pouring is questionable.

Conclusions

A more accurate solution to the problem was obtained by considering the temperature-dependent change in

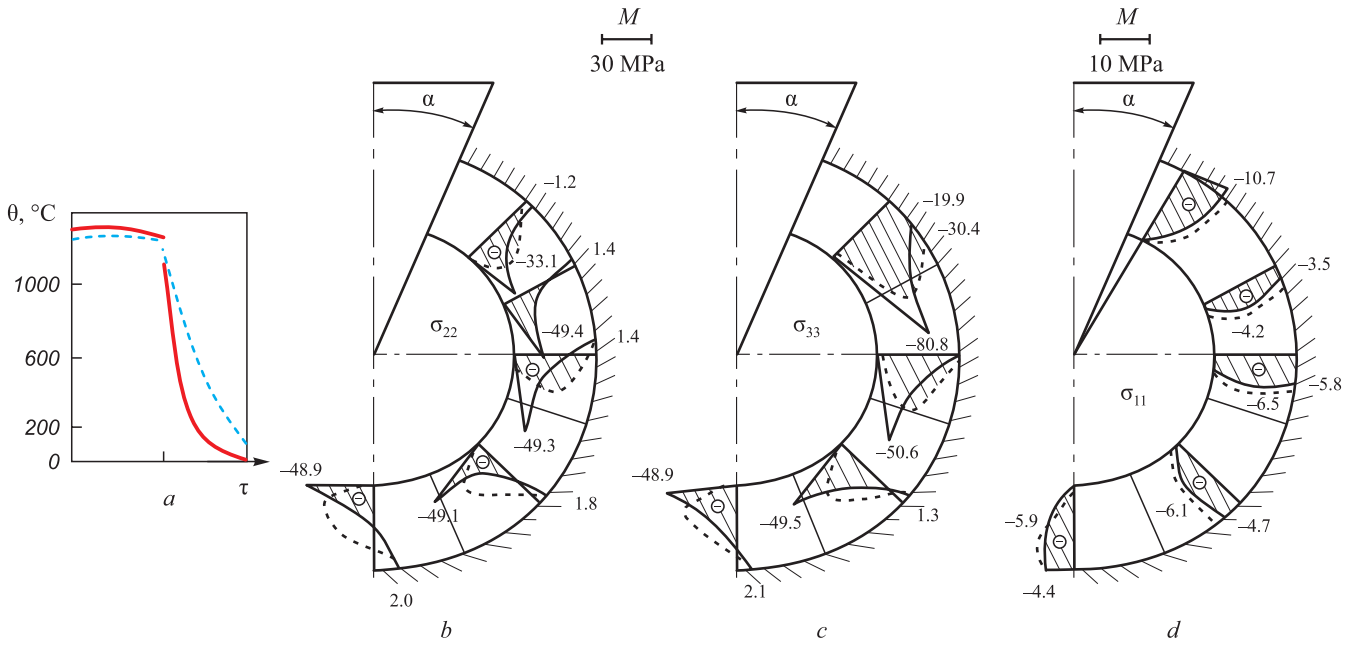

Fig. 8. Temperatures field (*a*), diagrams of normal stresses σ_{22} (*b*), σ_{33} (*c*) and σ_{11} (*d*) at α = 30° after casting cooling for 1.12 s (——) and 7.12 s (– – –)

Рис. 8. Поле температур (*a*), эпюры нормальных напряжений σ_{22} (*b*), σ_{33} (*c*) и σ_{11} (*d*) в ОФ при α = 30° через время охлаждения отливки 1,12 с (——) и 7,12 с (– – –)

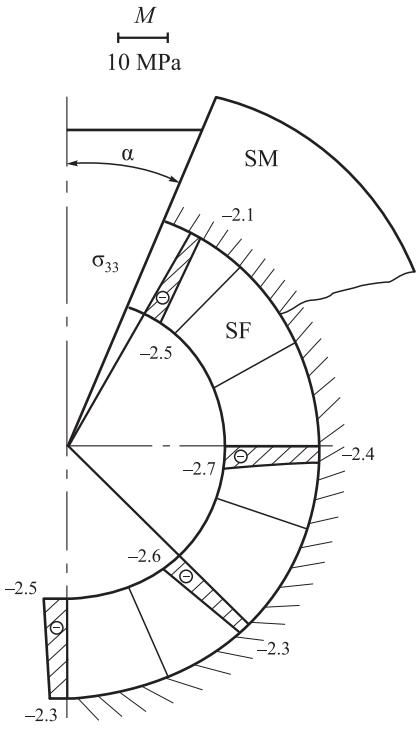

Fig. 9. Diagrams of normal stresses σ_{33} in formed metal crust after casting cooling for 7.12 s (α = 30°)

Рис. 9. Эпюры нормальных напряжений σ_{33} в образующейся корочке металла через время охлаждения отливки 7,12 с (α = 30°)

the shear modulus of the mold material, which significantly impacted the results. The analysis of the SSS in a spherical SM during the pouring of a steel casting showed that compressive stresses σ_{22} and σ_{33} at the interface between the SM and the liquid metal at the initial cooling stage are critical. Significant compressive stresses σ_{11} (up to 10 MPa) at the interface between the SM and the SF indicate the possibility and necessity of further theoretical study of this process by modeling the surface coverage area of the SF.

References / Список литературы

1. Bansode S.N., Phalle V.M., Mantha S.S. Optimization of process parameters to improve dimensional accuracy of investment casting using Taguchi approach. *Advances in Mechanical Engineering*. 2019;11(4):1–12. https://doi.org/10.1177/1687814019841460
2. Mittal Y.G., Kamble P., Gote G., Patil Y., Patel A. K., Bernard A., Karunakaran K.P. Mathematical modelling of pattern sublimation in rapid ice investment casting. *International Journal of Metalcasting*. 2022;16(2):1002–1009. http://dx.doi.org/10.1007/s40962-021-00665-w
3. Kanyo J.E., Schafföner S., Uwanyuze R.Sh., Leary K.S. An overview of ceramic molds for investment casting of nickel superalloys. *Journal of the European Ceramic Society*. 2020;40(15):4955–4973. https://doi.org/10.1016/j.jeurceramsoc.2020.07.013
4. Rafique M.M.A., Iqbal J. Modeling and simulation of heat transfer phenomena during investment casting. *International Journal of Heat and Mass Transfer*. 2009;52(7–8):2132–2139. http://doi.org/10.1016/j.ijheatmasstransfer.2008.11.007
5. Singh R. Mathematical modeling for surface hardness in investment casting applications. *Journal of Mechanical Science and Technology*. 2012;26:3625–3629. http://dx.doi.org/10.1007/s12206-012-0854-0

6. Jafari H., Idris M. H., Ourdjini A. Effect of thickness and permeability of ceramic shell mould on in situ melted AZ91D investment casting. *Applied Mechanics and Materials*. 2014;465–466:1087–1092. http://dx.doi.org/10.4028/www.scientific.net/AMM.465-466.1087

7. Bansode S.N., Phalle V.M., Mantha S. Taguchi approach for optimization of parameters that reduce dimensional variation in investment casting. *Archives of Foundry Engineering*. 2019;19(1):5–12. https://dx.doi.org/10.24425/afe.2018.125183

8. Pattnaik S., Karunakar D.B., Jha P.K. Developments in investment casting process – A review. *Journal of Materials Processing Technology*. 2012;212(11):2332–2348. https://doi.org/10.1016/j.jmatprotec.2012.06.003

9. Zhang J., Li K.W., Ye H.W., Zhang D.Q., Wu P.W. Numerical simulation of solidification process for impeller investment casting. *Applied Mechanics and Materials*. 2011;80–81: 961–964. https://doi.org/10.4028/www.scientific.net/AMM.80-81.961

10. Dong Y.W., Li X.L., Zhao Q., Jun Y., Dao M. Modeling of shrinkage during investment casting of thin walled hollow turbine blades. *Journal of Materials Processing Technology*. 2017;244:190–203. https://doi.org/10.1016/j.jmatprotec.2017.01.005

11. Rakoczy Ł., Cygan R. Analysis of temperature distribution in shell mould during thinwall superalloy casting and its effect on the resultant microstructure. *Archives of Civil and Mechanical Engineering*. 2018;18(4):1441–1450. https://doi.org/10.1016/j.acme.2018.05.008

12. Yameng W., Zhigang L. The design of testing methods for strength of ceramic shell mold in investment casting. *Proceedings of the Asia-Pacific Conf. on Intelligent Medical 2018 & Int. Conf. on Transportation and Traffic Engineering*. 2018;336–341. https://doi.org/10.1145/3321619.3321686

13. Kolczyk J., Zych J. High temperature strength of ceramic moulds applied in the investment casting method. *Archives of Foundry Engineering*. 2011;11(3):121–124.

14. Anglada E., Meléndez A., Maestro L., Domínguez I. Finite element model correlation of an investment casting process. *Materials Science Forum*. 2014;797:105–110. http://dx.doi.org/10.4028/www.scientific.net/MSF.797.105

15. Liu C., Sun J., Lai X., He B., Li F. Influence of complex structure on the shrinkage of part in investment casting process.*The International Journal of Advanced Manufacturing Technology*. 2015;77:1191–1203. https://doi.org/10.1007/s00170-014-6523-y

16. Liu C., Wang F., Jin S., Li F., Lai X. Permafrost analysis methodology (PAM) for ceramic shell deformation in the firing process. *International Journal of Metalcasting*. 2019;13(4):953–968. http://dx.doi.org/10.1007/s40962-019-00317-0

17. Everhart W.A., Lekakh S.N., Richards V., Chen J., Li H., Chandrashekhara K. Corner strength of investment casting shells. *International Journal of Metalcasting*. 2013;7:21–27. https://doi.org/10.1007/BF03355541

18. Sabau A.S. Numerical simulation of the investment casting process. *Transactions of American Foundry Society*. 2005;113:407–417.

19. Zheng K., Lin Y., Chen W., Liu L. Numerical simulation and optimization of casting process of copper alloy water-meter shell. *Advances In Mechanical Engineering*. 2020;12(5):1–12. http://dx.doi.org/10.1177/1687814020923450

20. Manzari M.T., Gethin D.T., Lewis R.W. Optimisation of heat transfer between casting and mould. *International Journal of Cast Metals Research*. 2000;13(4):199–206. https://doi.org/10.1080/13640461.2000.11819402

21. Rafique M.M.A., Shah U. Modeling and simulation of heat transfer phenomenon related to mold heating during investment casting. *Engineering*. 2020;12(5):291–314. http://dx.doi.org/10.4236/eng.2020.125024

22. Dong Y., Bu K., Zhang D. Numerical simulation of displacement field of solidification process for investment casting. In: *2008 Asia Simulation Conf. – 7th Int. Conf. on System Simulation and Scientific Computing*. 2008:715–720. https://doi.org/10.1109/asc-icsc.2008.4675453

23. Upadhya G.K., Das S., Chandra U., Paul A.J. Modelling the investment casting process: a novel approach for view factor calculations and defect prediction. *Applied Mathematical Modelling*. 1995;19(6):354–362. https://doi.org/10.1016/0307-904X(95)90001-O

24. Khan M.A.A., Sheikh A.K. Simulation tools in enhancing metal casting productivity and quality: A review. *Proceedings of the Institution of Mechanical Engineers, Part B: Journal of Engineering Manufacture*. 2016;230(10):1799–1817. https://doi.org/10.1177/0954405416640183

25. Banerjee S., Sutradhar G. Analysis of casting defects in investment casting by simulation. *Advances in Materials, Mechanical and Industrial Engineering: Selected Contributions from the First Int. Conf. on Mechanical Engineering, Jadavpur University, Kolkata, India*. Springer International Publishing. 2019:247–271. http://dx.doi.org/10.1007/978-3-319-96968-8_12

26. Одиноков В.И., Евстигнеев А.И., Дмитриев Э.А., Намоконов А.Н., Евстигнеева А.А., Чернышова Д.В. Напряженно-деформированное состояние керамической оболочковой формы при формировании в ней стальной шарообразной отливки. Часть 1. *Известия вузов. Черная металлургия*. 2024;67(2):211–218. https://doi.org/10.17073/0368-0797-2024-2-211-218

27. Odinokov V.I., Evstigneev A.I., Dmitriev E.A., Namokonov A.N., Evstigneeva A.A., Chernyshova D.V. Stress-strain state of ceramic shell mold during formation of spherical steel casting in it. Part 1. *Izvestiya. Ferrous Metallurgy*. 2024;67(2):211–218. https://doi.org/10.17073/0368-0797-2024-2-211-218

Одиноков В.И., Прокудин А.Н., Сергеева А.М., Севастьянов Г.М. Свидетельство о государственной регистрации программы для ЭВМ № 2012111389. ОДИССЕЙ. Зарегистрировано в Реестре программ для ЭВМ 13.12.2012.

28. Odinokov V.I., Dmitriev E.A., Evstigneev A.I., Ivankova E.P. Certificate of state registration of the computer program No. 2021111121 "Program for mathematical modeling the optimization of choice of temperature of the support filler, material physical properties and structure of shell mold according to smelted models to increase its crack resistance when cooling the casting in it". Registered in the Register of Computer programs on 04.11.2021. (In Russ.).

Одиноков В.И., Дмитриев Э.А., Евстигнеев А.И., Иванкова Е.П. Свидетельство о государственной регистрации программы для ЭВМ № 2021111121 «Программа математического моделирования оптимизации выбора температуры опорного наполнителя, физических свойств материала и структуры оболочковой формы по выплав-

ляемым моделям для повышения ее трещиностойкости при охлаждении в ней отливки». Зарегистрировано в Реестре программ для ЭВМ 11.04.2021 г.

29. Evstigneev A.I., Odinokov V.I., Dmitriev E.A., Chernyshova D.V., Evstigneeva A.A., Ivankova E.P. On the crack resistance of a ceramic shell mold according to smelted models when a spherical steel casting solidifies in it. *Liteinoe proizvodstvo*. 2022;(9):22–25. (In Russ.).

Евстигнеев А.И., Одиноков В.И., Дмитриев Э.А., Чернышова Д.В., Евстигнеева А.А., Иванкова Е.П. О трещиностойкости керамической оболочковой формы по выплавляемым моделям при затвердевании в ней шарообразной стальной отливки. *Литейное производство*. 2022;(9):22–25.

30. Odinokov V.I., Kaplunov B.G., Peskov A.V., Bakov A.V. Mathematical Modeling of Complex Technological Processes. Moscow: Nauka; 2008:178. (In Russ.).

Одиноков В.И., Каплунов Б.Г., Песков А.В., Баков А.В. Математическое моделирование сложных технологических процессов. Москва: Наука; 2008:178.

Сведения об авторах / Information about the Authors

Валерий Иванович Одиноков, *д.т.н., профессор, главный научный сотрудник Управления научно-исследовательской деятельностью,* Комсомольский-на-Амуре государственный университет
ORCID: 0000-0003-0200-1675
E-mail: 79122718858@yandex.ru

Алексей Иванович Евстигнеев, *д.т.н., профессор, главный научный сотрудник Управления научно-исследовательской деятельностью,* Комсомольский-на-Амуре государственный университет
ORCID: 0000-0002-9594-4068
E-mail: diss@knastu.ru

Эдуард Анатольевич Дмитриев, *д.т.н., доцент, ректор,* Комсомольский-на-Амуре государственный университет
ORCID: 0000-0001-8023-316X
E-mail: rector@knastu.ru

Александр Николаевич Намоконов, *аспирант,* Комсомольский-на-Амуре государственный университет
ORCID: 0009-0003-9269-7713
E-mail: namokonovsasha@mail.ru

Анна Алексеевна Евстигнеева, *студент,* Комсомольский-на-Амуре государственный университет
ORCID: 0000-0003-0667-2468
E-mail: annka.ewstic@mail.ru

Дарья Витальевна Чернышова, *аспирант,* Комсомольский-на-Амуре государственный университет
ORCID: 0000-0001-5142-2455
E-mail: daracernysova744@gmail.com

Valerii I. Odinokov, *Dr. Sci. (Eng.), Prof., Chief Researcher of the Department of Research Activities,* Komsomolsk-on-Amur State University
ORCID: 0000-0003-0200-1675
E-mail: 79122718858@yandex.ru

Aleksei I. Evstigneev, *Dr. Sci. (Eng.), Prof., Chief Researcher of the Department of Research Activities,* Komsomolsk-on-Amur State University
ORCID: 0000-0002-9594-4068
E-mail: diss@knastu.ru

Eduard A. Dmitriev, *Dr. Sci. (Eng.), Assist. Prof., Rector,* Komsomolsk-on-Amur State University
ORCID: 0000-0001-8023-316X
E-mail: rector@knastu.ru

Aleksandr N. Namokonov, *Postgraduate,* Komsomolsk-on-Amur State University
ORCID: 0009-0003-9269-7713
E-mail: namokonovsasha@mail.ru

Anna A. Evstigneeva, *Student,* Komsomolsk-on-Amur State University
ORCID: 0000-0003-0667-2468
E-mail: annka.ewstic@mail.ru

Dar'ya V. Chernyshova, *Postgraduate,* Komsomolsk-on-Amur State University
ORCID: 0000-0001-5142-2455
E-mail: daracernysova744@gmail.com

Вклад авторов / Contribution of the Authors

В. И. Одиноков – научное руководство, анализ результатов исследований, редактирование и корректировка финальной версии статьи.
А. И. Евстигнеев – формирование концепции статьи, определение цели и задачи исследования, анализ результатов исследования, подготовка текста.
Э. А. Дмитриев – проведение расчетов, их анализ, подготовка и корректировка текста.
А. Н. Намоконов – проведение расчетов, подготовка библиографического списка, обработка графического материала.
А. А. Евстигнеева – проведение расчетов, подготовка текстового и графического материала.
Д. В. Чернышова – обработка расчетных результатов, подготовка графического материала.

V. I. Odinokov – scientific guidance, analysis of research results, editing and correction of the article final version.
A. I. Evstigneev – formation of the article concept, definition of the purpose and objectives of the study, analysis of research results, writing the text.
E. A. Dmitriev – conducting calculations and their analysis, writing and correction of the text.
A. N. Namokonov – conducting calculations, preparation of references, processing of graphic material.
A. A. Evstigneeva – conducting calculations, preparation of the text and graphic material.
D. V. Chernyshova – processing of calculated results, preparation of graphic material.

Поступила в редакцию 19.04.2024
После доработки 24.05.2024
Принята к публикации 25.05.2024

Received 19.04.2024
Revised 24.05.2024
Accepted 25.05.2024